Design, Development and Experimental Evaluation of a Thrust Vectoring Vortex Climbing Robot*

Andreas Papadimitriou, George Andrikopoulos, George Nikolakopoulos

Abstract— **In this article, a novel Thrust Vectoring Vortex Climbing Robot (TVV-CR) will be presented from a design development and experimental evaluation perspective. To the goal of providing an efficient and robust climbing robot design, with minimized weight and high permissible payload, a novel Electric Ducted Fan (EDF)-based actuation design is proposed for achieving simultaneous locomotion and adhesion via a controllable tilt mechanism, while excluding the need for active motorized wheels. Towards the development of the TVV-CR, the design and development stages will be presented in detail, while proposing a P-PI-based cascaded control structure for evaluating its overall properties. The efficiency of the suggested scheme will be evaluated by multiple experimental results indicating the robot's ability to follow randomly generated paths, while maintaining its adhesion under different surface inclinations.**

I. Introduction

The research area of Wall-Climbing robots (WCR) has steadily gained interest over the years as a promising approach to remote inspection and maintenance of big and hard to reach spaces. The development of reliable WCRs with high payload capabilities, which could incorporate inspection and repair equipment, would significantly cut maintenance costs in areas where manual inspection times are high and human safety might be compromised [1]. Many different approaches have been proposed for the WCRs' adhesion including magnetic, pneumatic, mechanical and material-based methods, and their locomotion including leg and wheel-based, sliding frames and sequential robotic structures [2]-[3]. All these methods have been tailored for specific surfaces (ferrous or non-ferrous, smooth or rough, flat or curved, different inclinations etc.) and specific applications, which pose a requirement on the needed payload, depending on the incorporated equipment [4].

A comparison based only on payload can be misleading, as the base weight and structure of every setup is, most of the times, a direct indicator of their performance and their limitations. Lightweight structures have been characterized by smaller payload capabilities [5] – [7] but versatile in terms of surfaces and operating conditions [8] – [9], while heavier and more bulky structures with multiple actuators [10] – [11], could carry more payload, but at a cost of power, efficiency, controllability and risk of causing damage on sensitive surfaces, which could render them unsuitable for analysis techniques like Non Destructive Testing (NDT) [12].

Specifically, this article is a continuation of the work presented in [13], [14], which introduced a Vortex Actuation System (VAS), for investigating the potential of Electric Ducted Fans (EDFs) as non-contact adhesion actuators, while providing a methodology for optimizing their adhesion performance. The proposed design led to a significant increase in adhesion-to-weight ratios of commercially available EDFs, reaching even at 250% of their maximum thrust-to-weight ratio, thus enabling their incorporation in WCRs for increased efficiency.

This study focuses on the design and development of a Thrust Vectoring Vortex Climbing Robot (TVV-CR) which utilizes the aforementioned EDF-based actuation design. To the goal of providing an efficient and robust design for an NDT compliant robot platform, with minimized weight and high performance, a novel EDF-enabled approach is proposed for achieving simultaneous locomotion and adhesion without the need of active motorized wheels. In addition, this article is contributing towards the preliminary evaluation of an autonomously controlled performance under experimental tests with surfaces of different inclinations.

The rest of this article is structured as follows. Section II presents the conceptual design details of the TVV-CR, while Section III presents the theoretical structure for controlling the adhesion and locomotion components, along with the utilized path generation algorithm. In Section IV, an overview of the developed TVV-CR prototype and the utilized setup components is provided. The experimental sequences performed for the evaluation of the TVV-CR prototype are presented and commented in Section V. Finally, discussion points and concluding remarks are provided in Section VI.

II. TVV-CR Conceptual Design

For our purpose, the TVV-CR setup was designed with the main goal of minimizing the structure weight while maximizing performance and supported payload. Specifically, the incorporation of a single tilting-EDF was considered, which would allow the control of the EDF's angle to utilize its generated thrust for adhesion and locomotion at the same time, which with the incorporation of the VAS methodology presented in [14] could lead to a significant increase in overall adhesion performance. This alteration would render any motors for wheel actuation redundant, thus effectively reducing the weight and excluding any disadvantages of motorized wheels such as wheel slippage during movement.

The formulated design for the TVV-CR is being presented in Fig. 1, with highlighted properties and

*This work has received funding from the European Union's H2020 Framework Programme under the call FET-OPEN, grant agreement No. 665238.

The authors are with the Robotics Team and the Department of Computer Science, Electrical and Space Engineering at Luleå University of Technology, Luleå, Sweden

Corresponding Author's email: geoand@ltu.se

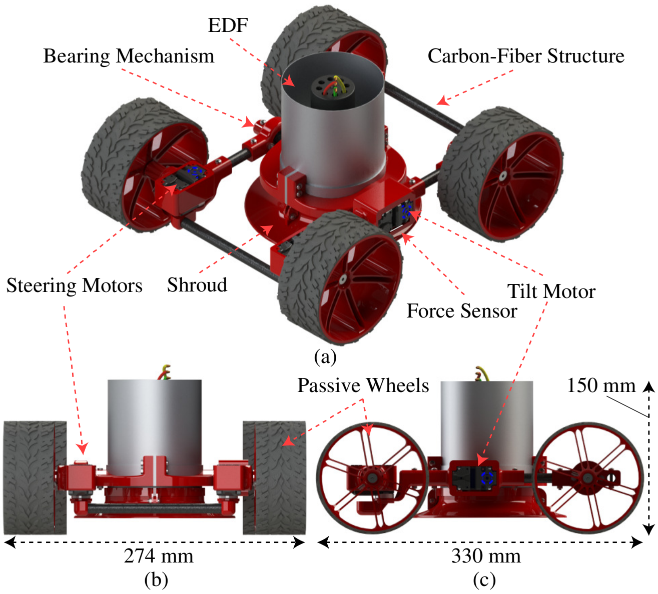

Fig. 1. Graphical representation of the TVV-CR setup: (a) isometric, (b) front and (c) side view with highlighted design properties and indicative dimensions.

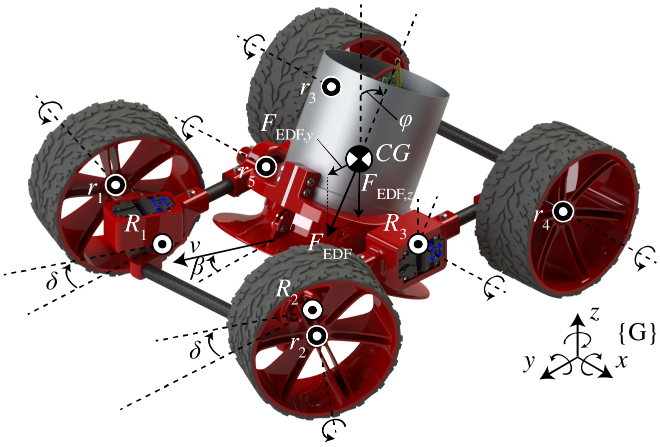

Fig. 2. Overview of the TVV-CR degrees-of-freedom (DOFs) and main geometrical components.

dimensions. Specifically, the proposed concept utilizes an EDF placed in the middle of a carbon-fiber-based structure, with the ability to rotate via a single motor, hereafter referred to as "tilt motor", with a bearing-based connector enabling rotation on the opposite side of the structure. The design includes four passively rotating wheels, via similar bearing connections, while only two, hereafter referred to as "front wheels", act as steering wheels via motor-enabled rotation.

As highlighted in this figure, the shroud mounted on the EDF via ring connectors and was properly placed to have the optimal distance [14] from the target surface in the state where the EDF is at zero tilt angle. As far as the sensing points are concerned, the structure has been designed to incorporate smart servo-motors capable of providing position/velocity feedback, while to enable the force measurement exerted from the EDF, a force sensing resistor has been properly placed between the tilt motor and its connector, to provide a single measuring point that could be translated to the total EDF force.

As defined in Fig. 2, the TVV-CR design is characterized by five passively rotating joints and three active rotational joints denoted as denoted as r_i, $i = 1, \ldots, 5$, and R_j, $j = 1,\ldots,3$. Specifically, $r_1 - r_4$ joints allow the rotation of the four passive wheels, while r_5 stabilizes the rotation of the EDF. The active R_1 and R_2 are responsible for steering the wheels at an angle δ from the y axis of the local frame {G} and R_3 enables the tilting of the EDF at an angle φ from the z axis.

The exerted EDF force vector F_{EDF} can by analyzed to its two components $F_{EDF,y}$ and $F_{EDF,z}$, in the respective y-z axes: a) $F_{EDF,z}$ being responsible for generating the adhesion to the target surface, while b) $F_{EDF,z}$ is the force component generating the linear motion of the robot which can be steered via the two R_1 and R_2 joints. When placed on top of a target surface, this configuration enables the TVV-CR motion with velocity v at a direction angle β from the y axis, while remaining attached despite changes in surface inclinations. The proposed design approach led to a 0.33 × 0.27 × 0.15 m (L × W × H) structure with a weight estimated on approximately 1.75 kg.

The adhesion and locomotion performance of the TVV-CR design was preliminarily assessed via simulation tools, which generated dynamically accurate responses. An iterative procedure of alternating design parameters provided an estimation of maximum payload performance at 2.14 kg for the robot to successfully operate on surfaces independently of the inclination, which reached up to 4.3 kg in the upside-down surface scenario by using the proposed methodology.

III. Control Scheme for Adhesion/Locomotion

A. *P-PI Based Cascaded Control Scheme*

The proposed TVV-CR design proposes a system characterized by a multiple-input-multiple-output (MIMO) structure, with the i) EDF throttle T, ii) EDF tilting φ and iii) steering wheel angles δ acting as the three defined inputs, while the a) generated EDF force F_{EDF}, b) vehicle velocity v, c) heading angle β and d) distance d from a desired point will be handled as the system outputs.

For the needs of providing a control base to validate the prototype's structural capabilities, a cascaded model-free control structure has been implemented and displayed in Fig. 3. The proposed scheme uses a combination of proportional (P) and proportional-integral (PI) controllers, formulated as in (1):

$$u_P(t) = K_P e(t), \quad u_{PI}(t) = K_P\left(e(t) + \frac{1}{T_I}\int_0^t e(t)\,dt\right), \qquad (1)$$

where K_P is the proportional gain and T_I the reset time in minutes. By an appropriate selection of the control parameters, the controllers' goal is to adjust the manipulated variable $u(t)$ and achieve minimization of the process' error signal $e(t) = SP(t) - PV(t)$, or equivalence between the Set-Point (SP) and Process Values (PV), while producing a system response within the designer's specifications.

For a given reference endpoint $d_{ref} = (x_{ref}, y_{ref})$ and the TVV-CR's current point $d = (x,y)$ in {O}, the proportional regulator P_1 is utilized for controlling the steering angle $\delta \in [\delta_{min}, \delta_{max}]$, through the heading angle error signal $e_\beta = \beta_{ref} - \beta$

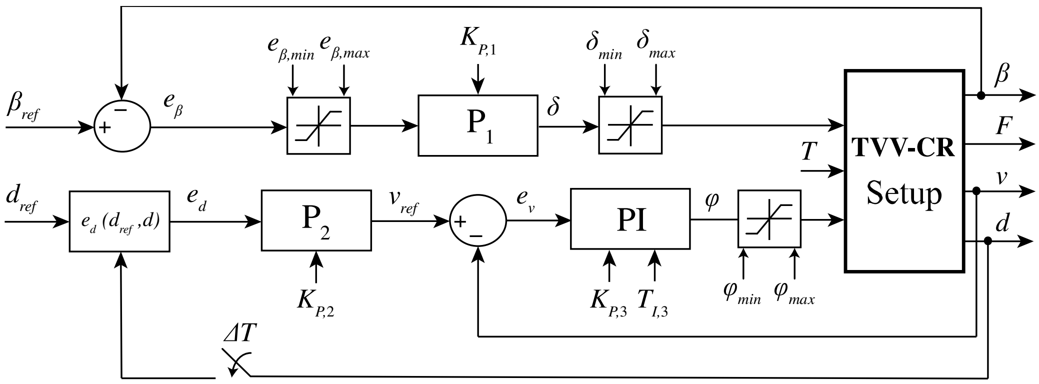

Fig. 3 Block diagram of the proposed cascaded P-PI-based control scheme.

$\in [e_{\beta,\min}, e_{\beta,\max}] = [-\pi, \pi]$, with the reference angle being denoted as:

$$\beta_{ref} = \arctan 2\left(\frac{y_{ref} - y}{x_{ref} - x}\right), \tag{2}$$

with arctan2(.) defining the angle in the Euclidean plane.

A cascaded proportional-integral (P_2-PI) controls the vehicle velocity v and distance d from a reference target point, with P_2 in the outer loop of the structure undertaking the control of the distance through the error defined as:

$$e_d = \sqrt{\left(x_{ref} - x\right)^2 + \left(y_{ref} - y\right)^2}, \tag{3}$$

and outputting the reference velocity v_{ref}. In turn, v_{ref} is fed into the PI controller of the inner loop via the velocity error $e_v = v_{\mathrm{ref}} - v$ and the control effort produced is the EDF tilt angle $\varphi \in [\varphi_{\min}, \varphi_{\max}]$.

It has to be noted that the coupled connection between the throttle T and tilting angle φ to the adhesion $F_{\mathrm{EDF},x}$ and locomotion $F_{\mathrm{EDF},y}$ force components has been simplified and the adhesion force has been considered as a feedforward relationship to the throttle input.

B. Path Generation

For evaluating the TVV-CR prototype's ability to follow a predefined path on a flat plane motion scenario, a path generation algorithm based on k-keypoint Bezier curves has been implemented (Table I). The keypoints are provided offline for the generation of the paths and their extracted n points are given as reference coordination to the TVV-CR.

TABLE I. PATH GENERATION ALGORITHM

1: Select k points in global {O} $p_k = (x_k, y_k)$ with $k \in \mathbb{R}$
2: Generate a linearly spaced n-sized vector in range [0, 1] $\rightarrow \vec{i} = linspace(0,1,n)$ that contains the path points
3: Generate the active point from the $(k\text{-}1)^{\mathrm{th}}$-order equation
$p(\vec{i}) = (1-\vec{i})^{k-1} * p_1 + c_1 (1-\vec{i})^{k-2} \vec{i} * p_2 + \ldots$ $\ldots + c_{k-2} (1-\vec{i}) \vec{i}^{k-2} * p_{k-1} + \vec{i}^{k-1} * p_k$
where $c_n \in \mathbb{R}$ for $n=[1,k]$ controls the curvature of the path and $*$ indicates the Kronecker tensor product.

The reference points are updated during operation, depending on the distance d between the current TVV-CR position and the i^{th} active point, while that update is governed by a tuned offset d_0. When the TVV-CR distance to the current active point becomes smaller than the offset ($d < d_0$), then the $(i+1)^{\mathrm{th}}$ point is activated. This process continues until the TVV-CR reaches the path's end-point.

IV. PROTOTYPE DEVELOPMENT AND SETUP COMPONENTS

The TVV-CR prototype, which is displayed in Fig. 4, was 3D printed from Polylactide (PLA) in Ultimaker 2+ printers, while its dimensions and mechanical details were a direct transfer from the conceptual design presented in Section II. For the preliminary evaluation presented in the next Section and as depicted in Fig. 4 a tethered rendition of the robot was implemented, where the power supply and parts of the micro-processing and data acquisition equipment were not mounted directly on the TVV-CR structure.

The EDF incorporated in this design was developed by Hobbyking (under the brand name Dr. MadThrust) and incorporating a 12-blade fan and a brushless DC motor 1600 kV with 3.8 kg maximum thrust. The specific model led to a 161% increase in its adhesion-to-weight ratio with the proposed methodology [14], while remaining more robust in its performance and less susceptible to resonant frequencies. The EDF's shroud was swapped during the experimental trials presented in Section V between its pre-built aluminium and a 3D printed rendition with outer radius 80 mm, following an outward curvature profile and constant shroud thickness 2 mm, and height 22 mm. The shroud was properly designed and placed to have the optimal distance from the test surface (15 mm, as extracted from [13]) for zero EDF tilt angle ($\varphi = 0°$).

The Electronic Speed Controller (ESC) selected for the tested EDF was the Turnigy AE-100A with continuous

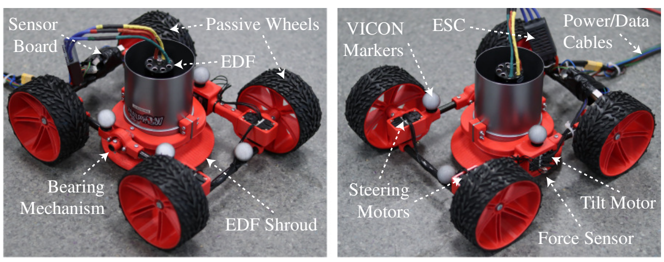

Fig. 4. TVV-CR prototype with highlighted setup components.

current capability of 100 A and characterized by a fast and precise throttle response. To handle the high maximum current requirements of the selected EDF, a EA-PSI 8080-70 2U power supply was selected, with the ability of providing output voltages (0-720V) and currents (0-120A).

For the steering and tilting functions of the TVV-CR, three HerkuleX DRS-0101 servo motors were selected for their specifications, given that they provide position and velocity feedback, while supporting position control at a 0 – 320° range and velocity control at continuous rotation mode with maximum speed at 360°/sec. The stall torque is estimated at 12 kg.cm. For measuring the force F_{EDF} generated from the EDF and acting on the test surface via the wheeled structure, a FlexiForce A401 force sensing resistor was placed between the EDF tilt motor and the plastic cover.

For the localization of the TVV-CR system during the preliminary experimental evaluation the VICON motion capturing system was utilized, which ensured high-accuracy measurements, with translation accuracy of approximately 0.04 mm and a respective angular accuracy of 0.02 degrees. The static friction constant between the test surface and the rubber on the TVV-CR wheels was experimentally measured at μ = 0.53. Finally, the acquisition of the setup's sensorial data and the control of the EDF's operation was achieved via one National Instruments USB-6008 cards and two Arduino Mega boards, while the main control and programming of the setup was performed in a personal computer system (Windows 7, 64-b, Intel i7 processor, 32-Gb RAM).

V. Experimental Evaluation

A. Evaluation Specifics

For the experimental evaluation of the TVV-CR properties multiple open and closed-loop trials were performed for different surface inclinations θ (Fig. 5). The experimental cases presented in the sequel were performed with the goal to analyse the relations among the position (x, y), velocity v and force F_{EDF} related to the throttle T, steering δ and tilt angle θ inputs, while evaluating the efficiency of the P-PI cascaded control structure presented in Section III.

For this preliminary evaluation of the TVV-CR, the throttle T input signal was selected at specific values tuned by open-loop experiments to ensure the robot's successful adhesion performance, with the program sampling frequency being set at 25 Hz. The acquired single-point force measurement was properly calibrated to provide an indication of the adhesion force component $F_{EDF,z}$, which was translated to the locomotion force component $F_{EDF,y}$ via the measurement of the EDF tilt angle φ and the use of their trigonometric relation $F_{EDF,y} = F_{EDF,z} \tan(\theta)$. The position ($x$,$y$) and the respective planar velocity v were acquired via the VICON motion capturing system and were provided on the local coordinate system {G}, while the feedback signals for the steering δ_i, with i=1,2 denoting the left and right steering motor as shown in Fig. 2, and tilt angle φ have been provided via the utilized Smart Servo Motors.

To investigate the full potential of utilizing the EDF as a tilting actuator for adhesion and locomotion, all cases have been executed with shrouds allowing a maximum tilt, while

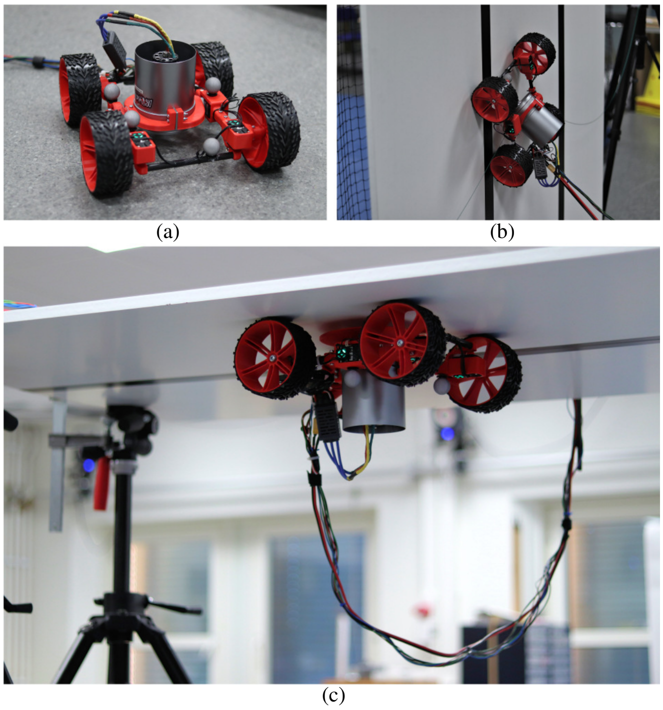

Fig. 5. Photographic stills during the evaluation sequences of the TVV-CR while placed on a surface of variable inclinations θ = a) 0°, b) 90°, and c) 180°.

the more challenging cases (θ = 180°) incorporated the optimized shroud for evaluation of maximum adhesion performance and payload.

For safety purposes, software constraints were properly set on φ and δ angles to avoid any increased mechanical stress or damage of the TVV-CR components during experimentation. Specifically, the EDF mechanism was constrained in the range of [φ_{min}, φ_{max}] = [-12.73, 12.73]° for the optimal 80 mm shroud described in [14], while with the use of smaller shrouds the range was bounded at [-90, 90]°, at the expense of maximum adhesion force but with the gain of maximum locomotion force. Finally, the steering angle δ was bounded between [δ_{min}, δ_{max}] = [-19, 19]° for both wheels.

B. Experimental Results

The control parameters $K_{P,1}$, $K_{P,2}$, $K_{P,3}$ and $T_{I,3}$ of the P-PI cascaded control, as defined in Section III, were fine-tuned via the trial-and-error method for every different inclination case, with constant values being utilized for each execution. Other fine-tuned parameters were the distance offset d_0, as defined in Section III for the switching between path points, and the EDF throttle T, which remained in constant values set for each of the presented cases and was tuned to ensure successful adhesion. The aforementioned control parameter values, as fine-tuned for the presented inclination cases θ = 15°, and 180°, are presented in Table II.

TABLE II. Control Parameter Set for the Investigated Surface Inclination Cases

θ [°]	$K_{P,1}$	$K_{P,2}$	$K_{P,3}$	$T_{I,3}$ [min]	d_0 [cm]	T [%]
15°	100	0.02	20	0.008	10	80
180°	70	0.03	20	0.01	6	60

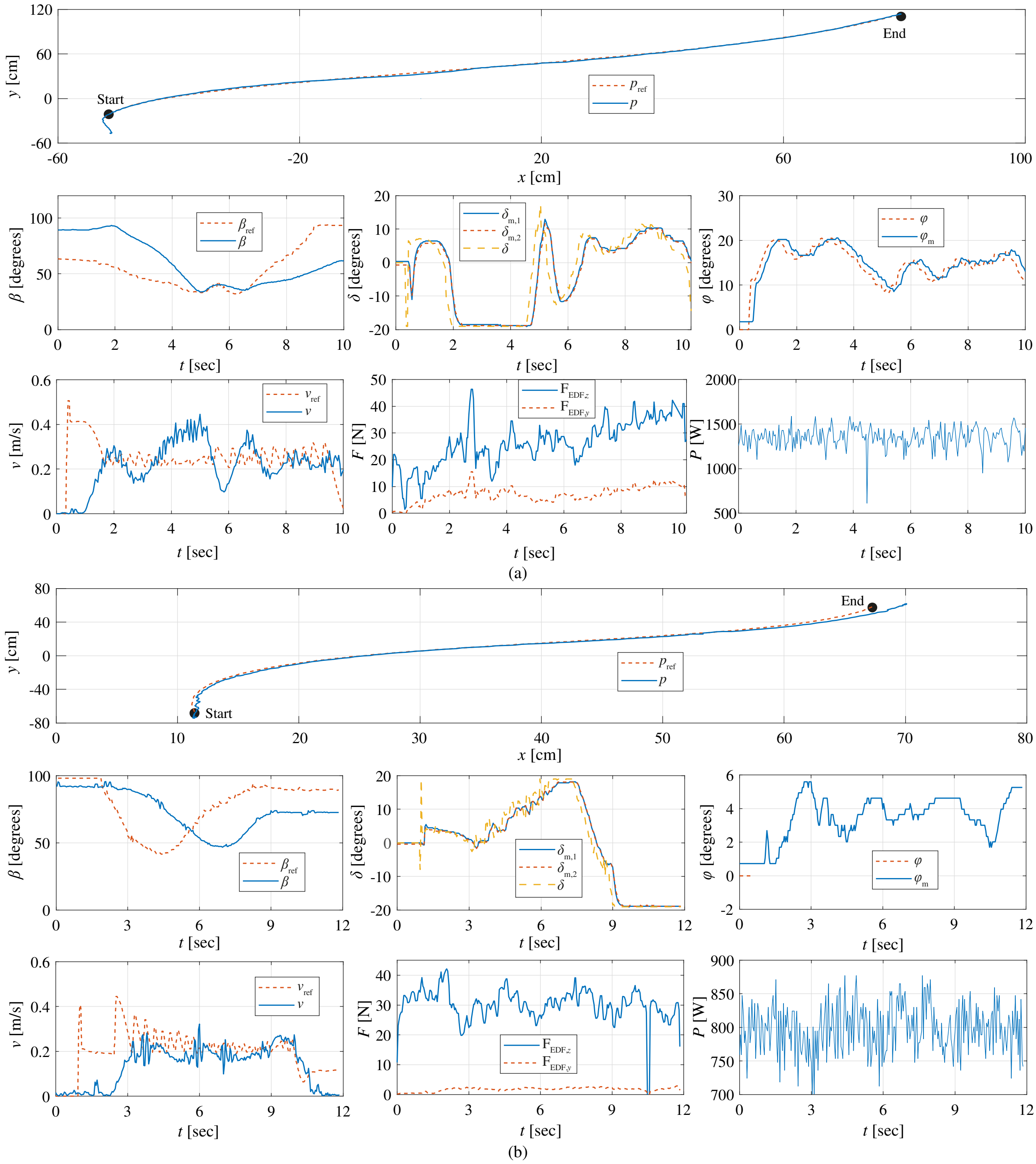

Fig. 6 TVV-CR path following response (x,y) for θ = (a) 15°, (b) 180° along with time responses of the heading angle β, the steering angles δ_1 and δ_2, EDF tilt angle φ, the vehicle planar velocity v, the EDF force components $F_{EDF,z}$ $F_{EDF,y}$, and drawn EDF power P.

The results including i) the path response $p = (x,y)$ in comparison to the reference path $p_{ref} = (x_{ref}, y_{ref})$, ii) the time response of the EDF tilt angle φ and the actual output from the tilt motor φ_m, iii) the angle responses $\delta_{m,1}$ and $\delta_{m,2}$ for the two steering motors in comparison to their angle command δ, iv) the vehicle planar velocity v response in comparison to the reference velocity v_{ref}, v) the EDF force components responsible for adhesion $F_{EDF,z}$ and locomotion $F_{EDF,y}$, and vi) the EDF power P drawn from the power supply, are presented in Fig. 6 (a) and (b), respectively.

For all investigated cases, the TVV-CR managed to successfully track the set paths defined for k = 4, while keeping adhesion in the case of non-zero inclinations. The path following responses were characterized by smooth motion and maneuvering, with the mean distance error remaining at low levels of approximately 3 cm. The largest error distances from the paths were identified in the cases where the path curvature exceeded the maneuvering capability of the TVV-CR, given the steering mechanical restriction, where the controller P_1 drove its output command δ to a saturated state. It must be noted that the steering motor responses $\delta_{m,1}$ and $\delta_{m,2}$ were handled by their internal PID controller and produced an accurate following of the reference signal.

Despite these saturations, the proportional control managed to track the reference heading angle β_{ref}, computed via (2), with δ commands that led the TVV-CR on the selected path. It can be observed that, for the inclined surfaces, P_1 controller produces a delayed β response, which highlights the coupled nature of the TVV-CR system, given that the specific response is directly affected by the velocity reference profile v_{ref} that is output from the second proportional controller P_2. The velocity profile, as expected, is characterized by a switching behavior due to $K_{p,2}$, while its tuning was properly adjusted so that it outputs a mean v_{ref} command in the order of 0.2 – 0.5 m/sec, depending on the inclination and desired performance.

The vehicle's planar velocity v is controlled by the PI controller, whose purpose is to output the tilt angle command φ to the TVV-CR, which is, in turn, was regulated by the internal PID control of the tilt servo motor providing the actual φ_{m} response. The PI control parameters were tuned with the purpose of providing a velocity response capable of converging to the mean value governed by the reference velocity signal.

The tilt operation altered the force component distribution depending on the needs for increasing the traction, adhesion or the speed. This coupled nature is presented via the responses of the adhesion component $F_{\text{EDF},z}$, which ensures the increased wheel traction in the most challenging cases, while the component $F_{\text{EDF},y}$ provides the linear motion.

As in the upside-down scenario (θ = 180°) a minimum adhesion force $F_{\text{EDF},z}$ of approximately 1.7 kg was required, equal to the weight of the TVV-CR, the required $F_{\text{EDF},y}$ for achieving motion was very small for overcoming the resulting low static friction. Similarly, in the tilted plane scenario (θ = 15°) $F_{\text{EDF},z}$ had to be minimal for increasing the traction given that no adhesion was required. The required locomotion forces increased significantly for increasing inclination values, while they became minimal in the upside-down case (θ = 180°) and maximal in the vertical θ = 90°.

For the case where θ = 180°, the use of the optimized shroud provides the needed force for fast movements, but most importantly an overall larger force bandwidth, which highly increases the maximum permissible payload to approximately 4.3 kg. In the case of θ = 15°, the EDF is equipped with a smaller in outer diameter shroud that enables the tilts necessary for the TVV-CR to develop the necessary $F_{\text{EDF},y}$. This ensured the successful locomotion in all cases but limited the permissible payload to a maximal value of approximately 2.1 kg in the case where θ = 90°, where the EDF is tilted close to φ = 90°, thus taking advantage of the full maximum free-flight thrust of approximately 3.8 kg.

VI. Conclusions

This article presented a Thrust Vectoring Vortex Climbing Robot (TVV-CR) from a design, development and experimental evaluation perspective. The work investigated the potential of utilizing the Electric Ducted Fan (EDF) as the core actuation for simultaneous locomotion and adhesion, referred to as Thrust Vectoring Vortex approach, to the goal of providing an efficient and robust design for the TVV-CR, with minimized weight and maximized performance for increased bandwidth and permissible payload. An iterative procedure of alternating design parameters provided a structure of 1.7 kg, while providing an estimated payload ranging from approximately 2.1 kg to 4.3 kg depending on the shroud usage and surface inclination. The platform was experimentally evaluated with the synthesis of a P-PI cascaded control algorithm, for tackling the multiple-input-multiple-output (MIMO) setup and the coupled input-output nature via path following tasks under surfaces of different inclinations. For all presented cases, the proposed TVV-CR system successfully managed to provide smooth and accurate responses, thus highlight the potential of utilizing such a system for future NDT inspection and repair tasks.

References

[1] Baeksuk Chu, Kyungmo Jung, Chang Soo Han, and Daehie Hong, "A survey of climbing robots: Locomotion and adhesion," *Int. J. Precis. Eng. Manuf.*, 11(4):633–647, 2010.

[2] A. Brusell, G. Andrikopoulos, G. Nikolakopoulos, "A Survey on Pneumatic Wall-Climbing Robots for Inspection", in *24th Mediterranean Conference on Control and Automation* (MED), 21 – 24 June 2016, Athens, Greece.

[3] G. Andrikopoulos, and G. Nikolakopoulos, "Vortex Actuation via Electric Ducted Fans: An Experimental Study," in Springer's Journal of Intelligent & Robotic Systems, 2018

[4] D. Schmidt and K. Berns, "Climbing robots for maintenance and inspections of vertical structures – A survey of design aspects and technologies," *Robotics and Autonomous Systems*, vol. 61, no. 12, pp. 1288-1305, 2013.

[5] VertiGo: A Wall-Climbing Robot including Ground-Wall Transition. 2015. https://www.vertigoproject.ch/

[6] D. Guan, L. Yan, Y. Yang, and W. Xu, "A Small Climbing Robot for the Intelligent Inspection of Nuclear Power Plants," *4th IEEE Int. Conf. Inf. Sci. Technol.*, 2014.

[7] S. Jung, J. Shin, W. Myeong, and H. Myung, "Mechanism and system design of MAV (Micro Aerial Vehicle)- type wall-climbing robot for inspection of wind blades and non-flat surfaces," *15th Int. Conf. Control. Autom. Syst.*, pages 1757–1761, 2015.

[8] Y. Tang, Q. Zhang, G. Lin, and J. Yin, "Switchable Adhesion Actuator for Amphibious Climbing Soft Robot," *Soft Robot.*, Jun. 2018.

[9] Y. Li, J. Krahn, and C. Menon, "Bioinspired Dry Adhesive Materials and Their Application in Robotics: A Review," *J. Bionic Eng.*, vol. 13, no. 2, pp. 181–199, 2016.

[10] Jianzhong Shang, Tariq Sattar, Shuwo Chen, and Bryan Bridge, "Design of a climbing robot for inspecting aircraft wings and fuselage," *Ind. Robot An Int. J.*, 34(6):495–502, 2007.

[11] Lufthansa Technik. Morfi. 2014.

[12] M. Al Rashed, M. Kimball, L. Vega, D. Vera, J. Soler, M. Correa, A. Garcia, G. S. Virk, and T. Sattar, "Climbing Robots for NDT Applications," in CLAWAR 2017: 20th International Conference on Climbing and Walking Robots and the Support Technologies for Mobile Machines, 11-13 September 2017, Porto, Portugal.

[13] A. Brusell, G. Andrikopoulos, G. Nikolakopoulos, "Novel Considerations on the Negative Pressure Adhesion of Electric Ducted Fans: An Experimental Study", in *25th Mediterranean Conference on Control and Automation* (MED), 3 – 6 July 2017, Valletta, Malta.

[14] G. Andrikopoulos, and G. Nikolakopoulos, "Design, Development and Experimental Evaluation of a Vortex Actuation System", in *14th IEEE/ASME International Conference on Mechatronic and Embedded Systems and Applications* (MESA), 2-4 July 2018, Oulu, Finland.